iScience

CellPress
OPEN ACCESS

Article

Streptococcus agalactiae and *Escherichia coli* induce distinct effector γδ T cell responses during neonatal sepsis

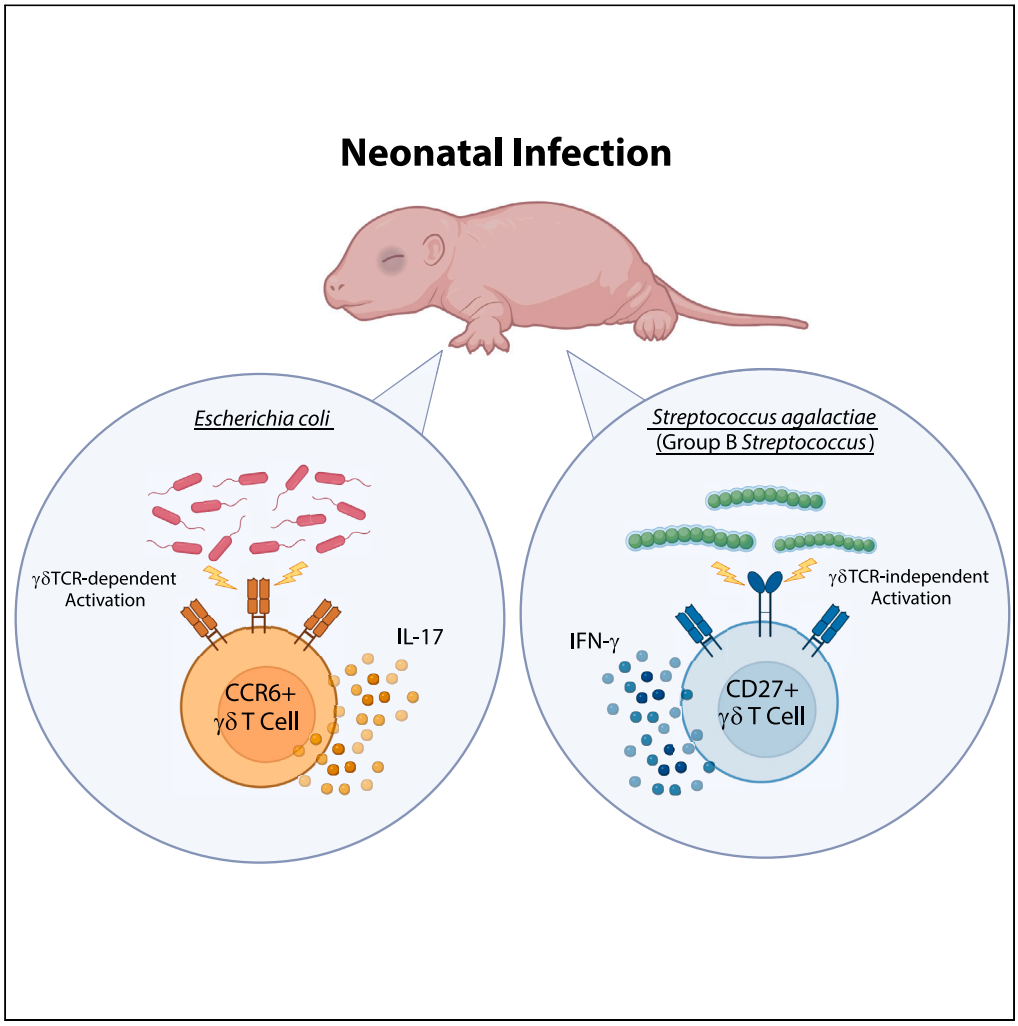

Lila T. Witt, Kara G. Greenfield, Kathryn A. Knoop

knoop.kathryn@mayo.edu

Highlights

γδ T cells in the neonate respond during group B *Streptococcus* and *Escherichia coli* sepsis

γδ T cells produce IFN-γ during GBS infection, and IL-17 during *E. coli* infection

GBS and *E. coli* neonatal infections induce unique neuroinflammatory phenotypes

γδ T cells impact sepsis-associated neuroinflammation in a pathogen-specific manner

Witt et al., iScience *27*, 109669
May 17, 2024
https://doi.org/10.1016/j.isci.2024.109669

iScience

CellPress
OPEN ACCESS

Article

Streptococcus agalactiae and *Escherichia coli* induce distinct effector γδ T cell responses during neonatal sepsis

Lila T. Witt,[1,2] Kara G. Greenfield,[1] and Kathryn A. Knoop[1,3,4,*]

SUMMARY

Neonates born prematurely are vulnerable to life-threatening conditions such as bacterial sepsis. *Streptococcus agalactiae* (GBS) and *Escherichia coli* are frequent causative pathogens of neonatal sepsis, however, it remains unclear if these pathogens induce differential immune responses. We find that γδ T cells rapidly respond to single-organism GBS and *E. coli* bloodstream infections in neonatal mice. Furthermore, GBS and *E. coli* induce distinct cytokine production from IFN-γ and IL-17 producing γδ T cells, respectively. We also find that IL-17 production during *E. coli* infection is driven by γδTCR signaling, whereas IFN-γ production during GBS infection occurs independently of γδTCR signaling. The divergent effector responses of γδ T cells during GBS and *E. coli* infections impart distinctive neuroinflammatory phenotypes on the neonatal brain. Thus, the neonatal adaptive immune system differentially responds to distinct bacterial stimuli, resulting in unique neuroinflammatory phenotypes.

INTRODUCTION

Premature neonates are acutely at risk for the development of life-threatening infections such as neonatal sepsis and meningitis.[1,2] Neonatal susceptibility to infection is not only facilitated by environmental factors such as prolonged stay in the neonatal intensive care unit (NICU) but also by the relative immaturity of the neonatal immune system.[1,3,4] Although the understanding of the neonatal immune system has progressed significantly over the past decade, how the neonatal adaptive immune system responds to disparate bacterial insults remains poorly understood.

Bloodstream infections preceding neonatal sepsis and meningitis can be caused by both gram-negative and gram-positive bacteria. *Escherichia coli* (*E. coli*) and *Streptococcus agalactiae* (group B *Streptococcus*; GBS) are among the most common causative pathogens implicated in neonatal bacterial sepsis.[5] Gram-negative bacilli such as *Klebsiella*, *Pseudomonas*, and *E. coli* are prevalent in the gastrointestinal tract of premature neonates and are capable of translocating from the gut and causing sepsis.[3,6,7] Increased bacterial translocation from the neonatal gut is facilitated in part by selective deficiencies in gut barrier defense mechanisms, including decreased production of protective factors such as mucous, anti-microbial peptides, and IgA.[6]

Conversely, gram-positive neonatal sepsis is frequently caused by *Staphylococcus aureus* and *Streptococcus agalactiae*, or group B *Streptococcus* (GBS). GBS colonizes the neonate via vertical transmission during birth, often as the result of the neonate aspirating GBS-infected amniotic fluid during parturition.[8] Although rates of GBS neonatal sepsis are declining due to improved early detection methods and prophylactic maternal antibiotic administration, the mortality rate of GBS neonatal sepsis can be as high as 10%, with 30–50% of survivors going on to experience neurological comorbidities in early childhood.[9]

Although both GBS and *E. coli* can be found as components of a healthy microbiota, they have the potential to cause severe disease in vulnerable populations, such as neonates.[10] The increased risk of sepsis development among preterm neonates is further compounded by deficiencies in several innate immunological defense mechanisms. Compared to adults, neonates have reduced complement proteins in their blood, impaired neutrophil function, and impaired secretion of pro-inflammatory cytokines by dendritic cells.[11] Similar to the innate immune system, the adaptive immune system in neonates bears several striking deficiencies to that of adults,[11] including a skewing of $CD4^+$ T cells toward Th2 over Th1 differentiation, further impairing the ability of neonates to mount a proper immune response to microbial infections.[12–14] Neonates also have deficiencies in humoral immunity, such as delayed germinal center formation and reduced antibody responses to both T cell-dependent and independent antigens.[15]

Despite their relative impairments in the conventional T and B cell compartments, neonates have a functional population of γδ T cells.[13] γδ T cells are innate-like lymphocytes that are abundant in barrier sites and act as early immune sentinels during infection.[16,17] In contrast to

[1]Department of Immunology, Mayo Clinic, Rochester MN 55901, USA
[2]Mayo Graduate School of Biomedical Sciences, Mayo Clinic, Rochester, MN 55901, USA
[3]Department of Pediatrics, Mayo Clinic, Rochester, MN 55901, USA
[4]Lead contact
*Correspondence: knoop.kathryn@mayo.edu
https://doi.org/10.1016/j.isci.2024.109669

conventional CD4$^+$ and CD8$^+$ T cells, γδ T cells are exported from the thymus as functionally mature cells and are poised to rapidly deploy their effector functions upon the detection of microbial ligands or pro-inflammatory cytokines.[18] As the first T cells to develop in the embryonic thymus,[19,20] γδ T cells are critical players in the neonatal immune response during a time when CD4$^+$ and CD8$^+$ T cells, and B cells are still developing and maturing.[17,21,22] Indeed, γδ T cells have been shown to play a critical role in host protection during neonatal influenza[23] and *Clostridium difficile* infection[24] underscoring their importance during early life.

In the present study, we characterize the immune responses to two major neonatal sepsis pathogens, *Streptococcus agalactiae* (Group B *Streptococcus*) and *Escherichia coli*. We report that these two pathogens induce distinct effector cytokine responses from γδ T cells in postnatal day 7 (P7) pups. We also report that these two pathogens drive distinct neuroinflammatory phenotypes in neonatal mice and that γδ T cells contribute to sepsis-induced neuroinflammation in a pathogen-specific manner. This study sheds light on how distinct sepsis pathogens drive differential γδ T cell effector responses in neonatal mice.

RESULTS

γδ T cells respond to E. coli and GBS neonatal sepsis

While GBS and *Escherichia coli* are frequent causative pathogens of neonatal sepsis, it is still unclear if features of these bacteria differentially drive the neonatal adaptive immune response. Previous studies have suggested that GBS and *E. coli* may utilize different routes of entry to cause sepsis: neonatal GBS disease is often the result of vertical transmission *in utero* or during parturition[25,26]; however, clinical data have suggested that GBS can also disseminate from the gut to cause sepsis.[27] *E. coli* is also associated with enteric sepsis, as we and others have shown that *E. coli* can readily translocate from the neonatal intestine to cause sepsis.[3] Therefore, we intraperitoneally infected neonatal pups (postnatal day 7; P7) with a single-organism infection of either 10^6 CFU *Streptococcus agalactiae* (GBS) or 2×10^4 CFU *E coli* "bloodstream isolate B" (BSI-B) to directly compare the systemic response to these bacteria independent of the route of entry. Pups were sacrificed at 18 h post-infection, a time point at which sepsis-induced weight loss begins (data not shown), and the spleen was analyzed as a readout of the systemic inflammatory response to GBS and *E. coli* infection. Both *E. coli* and GBS septicemia induced robust activation of splenic γδ T cells 18 h post-infection, as measured by an increase in the proportion of activated (CD69$^+$ CD62L−) γδ T cells compared to uninfected controls (Figures 1A and 1B). A significant increase in the absolute number of activated γδ T cells during *E. coli* infection was also observed, along with a modest but statistically non-significant increase in the number of activated γδ T cells during GBS infection (Figure 1C). In addition to the γδ T cell compartment, a slight increase in the activation status of conventional CD4$^+$ and CD8$^+$ T cells, and B cells was also observed (Figures S1A–S1C). Therefore, these data show that γδ T cells in the neonate rapidly respond to both *E. coli* and GBS infection.

E. coli and GBS neonatal sepsis drive distinct effector cytokine responses from γδ T cells

We next sought to further characterize the responses of γδ T cells during GBS and *E. coli* neonatal sepsis. γδ T cells undergo developmental programming in the thymus and exist in the periphery as either IL-17 or IFN-γ producers.[18,28,29] We therefore asked which γδ T cell effector cytokine profiles were being elicited during neonatal GBS and *E. coli* infection. Cytokine staining of total splenic γδ T cells revealed a robust increase in IL-17 expression during *E. coli*, but not GBS infection, whereas GBS infection induced increased IFN-γ, but not IL-17, expression from γδ T cells (Figures 2A–2C). These findings were validated with serum ELISA, showing global systemic increases in IFN-γ during GBS infection and IL-17 during *E. coli* infection (Figures 2D and 2E). γδ T cell effector programs can also be discerned based on the expression of surface markers, such as CCR6, restricted to IL-17 producing γδ T cells, and CD27, restricted to IFN-γ producing γδ T cells. Accordingly, during GBS infection, there was an increase in the proportion of activated CD27$^+$ γδ T cells, but not CCR6+ γδ T cells compared to uninfected controls (Figure 2F). Conversely, during *E. coli* infection, there was an increase in the proportion of activated CCR6+ γδ T cells, but not CD27$^+$ γδ T cells compared to uninfected controls (Figure 2G). These data demonstrate that GBS neonatal sepsis drives the specific activation of CD27$^+$, IFN-γ-producing γδ T cells, whereas *E. coli* infection activates CCR6+, IL-17-producing γδ T cells, resulting in the induction of discrete effector cytokine programs.

E. coli neonatal infection drives pathogenic γδTCR signaling

γδ T cells are capable of undergoing activation via multiple pathways, including (Major histocompatibility complex) MHC-independent (T cell receptor) TCR activation by pathogen-derived non-peptide antigens.[30] Nur77 is a transcription factor that is rapidly and specifically expressed during antigen-receptor-mediated signaling and activation in T and B cells.[31,32] Therefore, we utilized P7 neonatal Nur77-GFP reporter pups to determine if γδTCR signaling occurs during GBS and *E. coli* sepsis. In the spleens of *E. coli*-infected pups 18 h post-infection, there was an increase in the proportion of Nur77+ CD69$^+$ γδ T cells (Figures 3A and 3B), indicating γδTCR-mediated activation. Importantly, nearly all Nur77+ CD69$^+$ γδ T cells expressed CCR6 (Figure 3C), suggesting that the IL-17 signature during *E. coli* neonatal sepsis is associated with γδTCR signaling. To gain insight into the nature of the *E. coli* antigen recognized by γδ T cells, we performed an *in vitro* culture of heat-killed (HK) *E. coli* BSI-B with Nur77-GFP splenocytes. Culture with HK *E. coli* BSI-B was sufficient to increase the proportion of Nur77+ CD69$^+$ γδ T cells (Figures S2A and S2B), suggesting that live *E. coli* is not required for neonatal γδTCR activation. We next sought to determine if γδTCR signaling during *E. coli* infection impacts IL-17 production and survival. To this end, we treated pups with 15 μg/g anti-TCRγδ UC7-13D5 antibody (Figure S3A), which has been shown to induce internalization of the γδTCR *in vivo*.[33] The use of a second anti-γδTCR antibody confirmed the γδTCR was not expressed in the spleen or liver upon treatment with the UC7-13D5 antibody (Figure S3B). Importantly, treatment with this antibody during *E. coli* infection was sufficient to decrease the production of IL-17 (Figure 3D), confirming that IL-17 production during *E. coli*

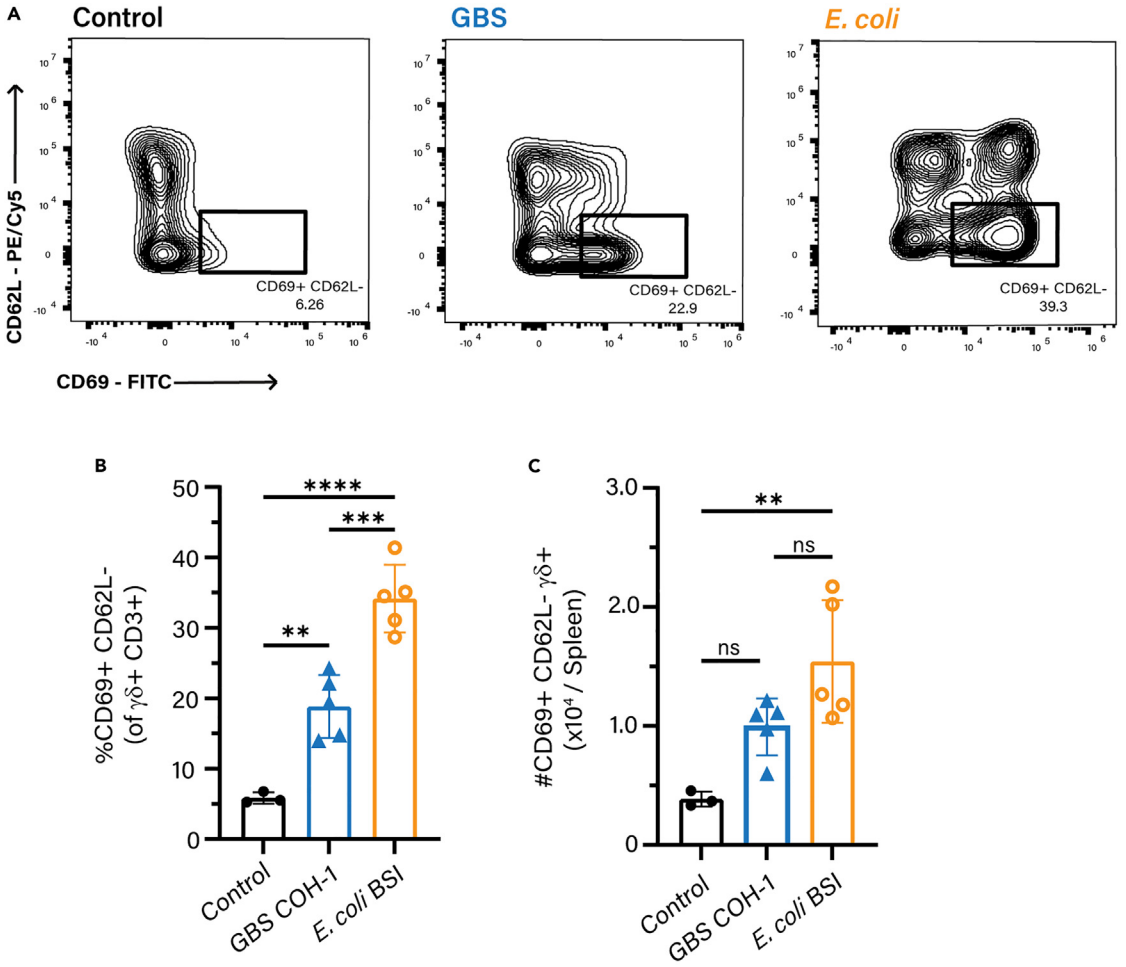

Figure 1. γδ T cells respond to *E. coli* and GBS neonatal sepsis

BL/6 pups were infected with GBS or *E. coli* on P7, and the spleen was analyzed 18 h post-infection.

(A) Gating scheme, (B) frequency, and (C) absolute number of CD69$^+$, CD62L-splenic γδ+ T cells. The data shown is from four independent experiments with $n > 3$ mice per group, where each dot represents one mouse. Controls are uninfected age-matched littermates. Statistical tests used include one-way ANOVA (B and C). ns = $p > 0.05$, ** = $p \leq 0.01$, *** = $p \leq 0.001$, **** = $p \leq 0.0001$.

infection is driven by γδTCR signaling. Blockade of the γδTCR in *E. coli*-infected pups was sufficient to rescue mortality independent of bacterial burden (Figures 3E and 3F), however, TCRδ−/− pups, which are devoid of a γδ T cell population, rapidly succumb to *E. coli* infection, despite similar bacterial burden to isotype and anti-TCRγδ-treated pups (Figures 3E and 3F).

Interestingly, there was no change in the proportion of Nur77+ CD69$^+$ γδ T cells in the spleens of GBS-infected pups (Figures 3A and 3B), suggesting TCR-independent activation of CD27$^+$ γδ T cells during GBS infection. As such, both blockade of the γδTCR, and global deletion of γδ T cells had no impact on survival or pathogen burden during GBS infection (Figures S3C and S3D). Therefore, we next asked if IFN-γ production from γδ T cells during GBS infection was driven by other cytokines in the inflammatory milieu. γδ T cells can produce IFN-γ in response to IL-12 and IL-18;[29,34] therefore, we tested the serum of GBS-infected pups for the presence of these cytokines. During neonatal GBS infection, no statistically significant increases in IL-12 or IL-18 were observed (Figures S4A–S4C), therefore, it is unlikely that IFN-γ production during GBS infection is driven by these cytokines. Overall, these data suggest that the CCR6+ IL-17+ γδ T cells responding to *E. coli* and CD27$^+$ IFN-γ+ γδ T cells responding to GBS neonatal sepsis undergo distinct pathways of activation to elicit effector cytokine production.

Neuroinflammation is a feature of E. coli and GBS neonatal sepsis

Adverse neurologic outcomes are associated with inflammatory events in early life, including bacterial sepsis.[9,35] We therefore sought to characterize the neuroinflammatory phenotypes associated with *E. coli* and GBS septicemia. Live *E. coli* and GBS were present in the brains of P7 pups 18 h post-infection (Figure 4A), suggesting neuroinflammation during neonatal sepsis is not the result of sterile inflammation, but is rather driven by live bacteria in the brain parenchyma. We next sought to characterize changes to immune cell populations in the neonatal

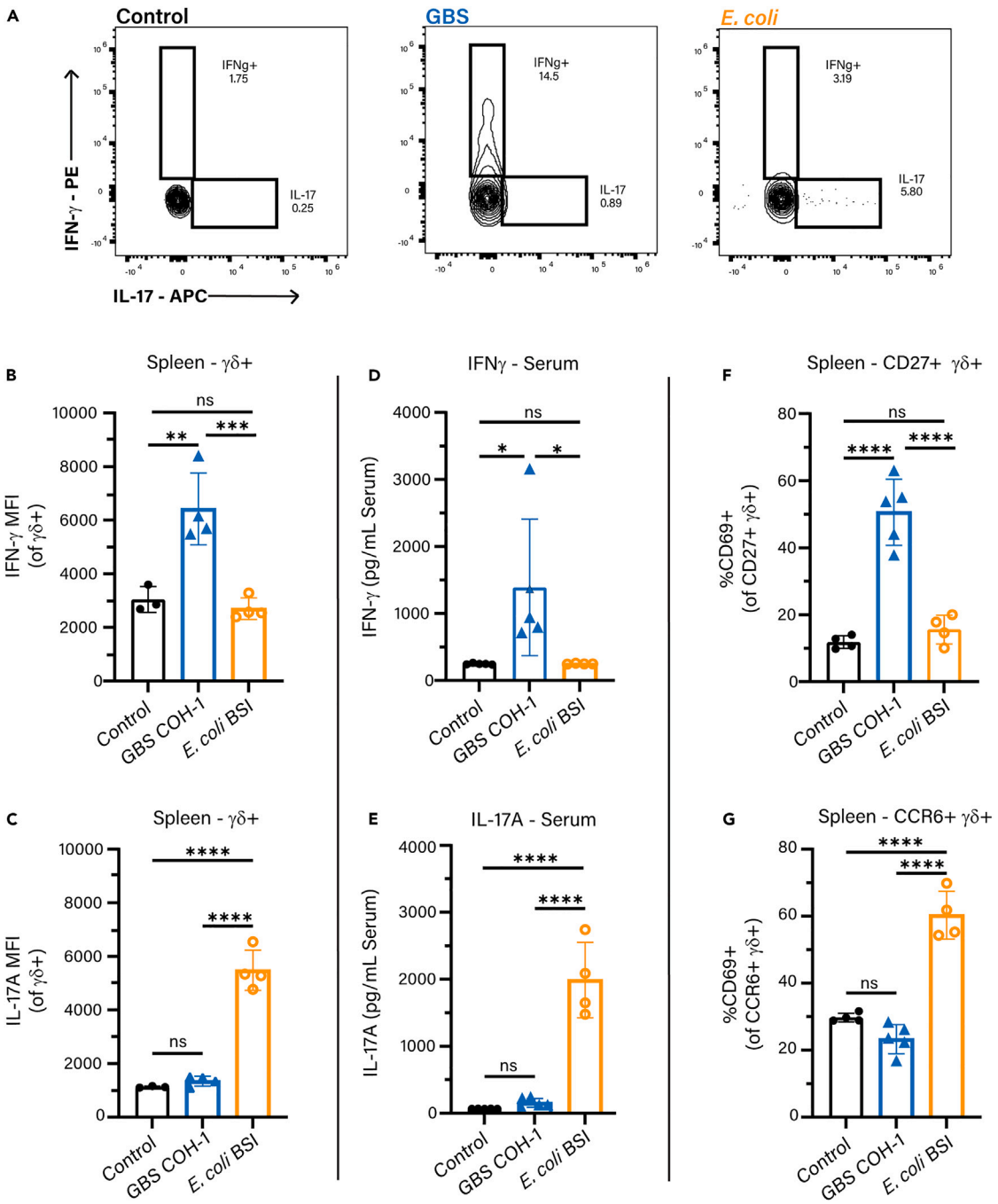

Figure 2. *E. coli* and GBS neonatal sepsis drive distinct effector cytokine responses from γδ T cells

BL/6 pups were infected with GBS or *E. coli* on P7, and the splenic and systemic cytokine response was measured 18 h post-infection.

(A) Flow cytometry gating scheme of IFN-γ+ and IL-17+ splenic γδ+ T cells 18 h post-infection.

(B) Mean fluorescent intensity (MFI) of IFN-γ and (C) IL-17 from total splenic γδ+ T cells 18 h post-infection.

(D) IFN-γ and (E) IL-17 serum ELISA 18 h post-infection, samples were pooled from infected pups from A and B.

(F) Proportion of activated CD27$^+$ and (G) CCR6+ γδ+ T cells from uninfected, GBS and *E. coli* infected BL/6 P7 pups 18 h post-infection. Data shown is from three independent experiments, $n > 3$ mice per group, where each dot represents one mouse. Uninfected age-matched littermates were used as controls. Statistical tests used include one-way ANOVA (B–G) with ns = $p > 0.05$, * = $p \leq 0.05$, ** = $p \leq 0.01$, *** = $p \leq 0.001$, **** = $p \leq 0.0001$.

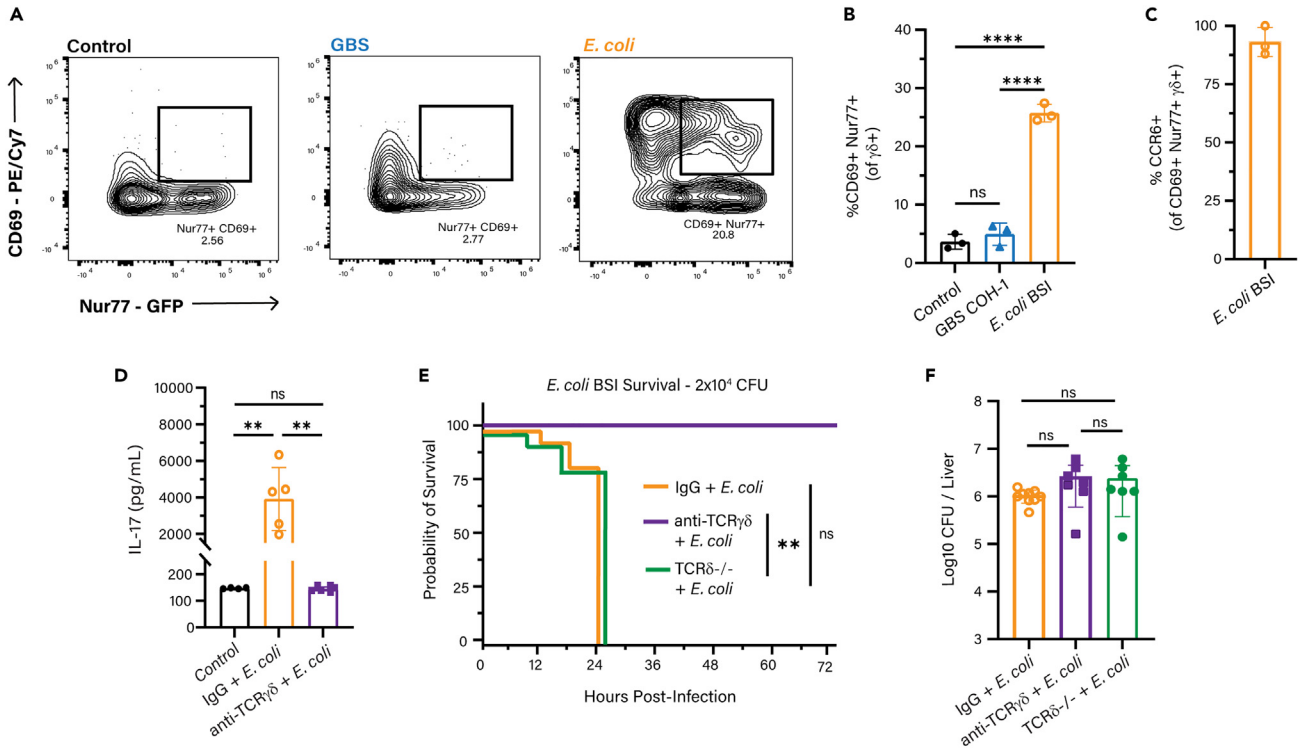

Figure 3. γδTCR signaling occurs during *E. coli*, but not GBS neonatal sepsis

Nur77GFP pups were infected with GBS or *E. coli* on P7 and spleens were harvested 18 h post-infection.

(A) Flow cytometry gating scheme, and (B) Quantification of CD69^{+} Nur77+ splenic γδ+ T cells from control, GBS-infected, and *E. coli*-infected pups.

(C) Percentage of CD69^{+} Nur77+ splenic γδ+ T cells from *E. coli* infected pups that express CCR6.

(D) IL-17 serum ELISA data from *E. coli*-infected pups treated with either isotype IgG or 15 μg/g anti-TCRγδ UC7-13D5 antibody.

(E) Survival curves and (F) Bacterial CFUs from the livers of *E. coli*-infected TCRδ−/− or BL/6 P7 pups treated with either isotype IgG or 15 μg/g anti-TCRγδ UC7-13D5 antibody. Controls are uninfected age-matched littermates. Data shown is from three independent experiments, $n > 3$ mice per group, where each dot represents one mouse. Statistical tests used include Kaplan-Meier (E), one-way ANOVA (B, D, F) with ns = $p > 0.05$, ** = $p \leq 0.01$, **** = $p \leq 0.0001$.

brain during GBS and *E. coli* infection. Flow cytometry analysis of CD45^{hi} immune cells in the perfused brains of P7 pups revealed a significant increase in monocytes and neutrophils in the brains of *E. coli*-infected pups compared to uninfected control pups and GBS-infected pups (Figures 4B, 4C, and S5). Interestingly, no significant increase in brain-infiltrating monocytes or neutrophils was noted in GBS-infected pups compared to control mice (Figures 4B and 4C).

To further investigate the neuroinflammatory phenotype associated with GBS and *E. coli* neonatal sepsis, we measured the mRNA of immunological genes from bulk brain tissue using the Nanostring nCounter gene expression platform (Table S1). In the brains of both GBS and *E. coli*-infected P7 pups, there was a significant increase in the expression of monocyte and neutrophil chemotactic factors, such as *Ccl2* and *Cxcl1*, respectively (Figures 4D and 4E). Compared to the brains of uninfected control mice, *E. coli*-infected pups had increased expression of genes associated with TLR4, such as *Cd14*, and the complement pathway, such as *C1ra*, *C3* (Figure 4D). Compared to uninfected pups, the brains of GBS-infected pups had increased expression of genes involved in the innate immune response to gram-positive bacteria, such as *Tlr1* and *MyD88* (Figure 4E). There were thirty-two differentially expressed genes between the brains of GBS and *E. coli*-infected pups including increased expression of *Casp-3* during GBS infection, and increased *Il23a* expression during *E. coli* infection (Figure 4F). Furthermore, principal component analysis (PCA) of Nanostring data revealed that *E. coli* and GBS-infected brains cluster distinctly from one another (Figure S6A). Overall, these findings indicate that although both GBS and *E. coli* can cause neuroinflammation during single-organism neonatal sepsis infection, they induce distinct inflammatory phenotypes in the neonatal brain.

γδ T cells differentially impact GBS and E. coli sepsis-associated neuroinflammation

Central nervous system (CNS)-resident γδ T cells are highly skewed toward IL-17 production and CCR6 expression at baseline[36,37] and play indispensable roles during homeostasis.[36,38] Under neuroinflammatory conditions, γδ T cells can have both protective[39] and pathogenic[40,41] effects on the CNS. Therefore, we sought to understand the contribution of γδ T cells to the neuroinflammatory phenotypes observed during GBS and *E. coli* neonatal sepsis. Similar to the spleen, we observed an increase in the proportion of Nur77+ CD69^{+} γδ T cells in the brain of

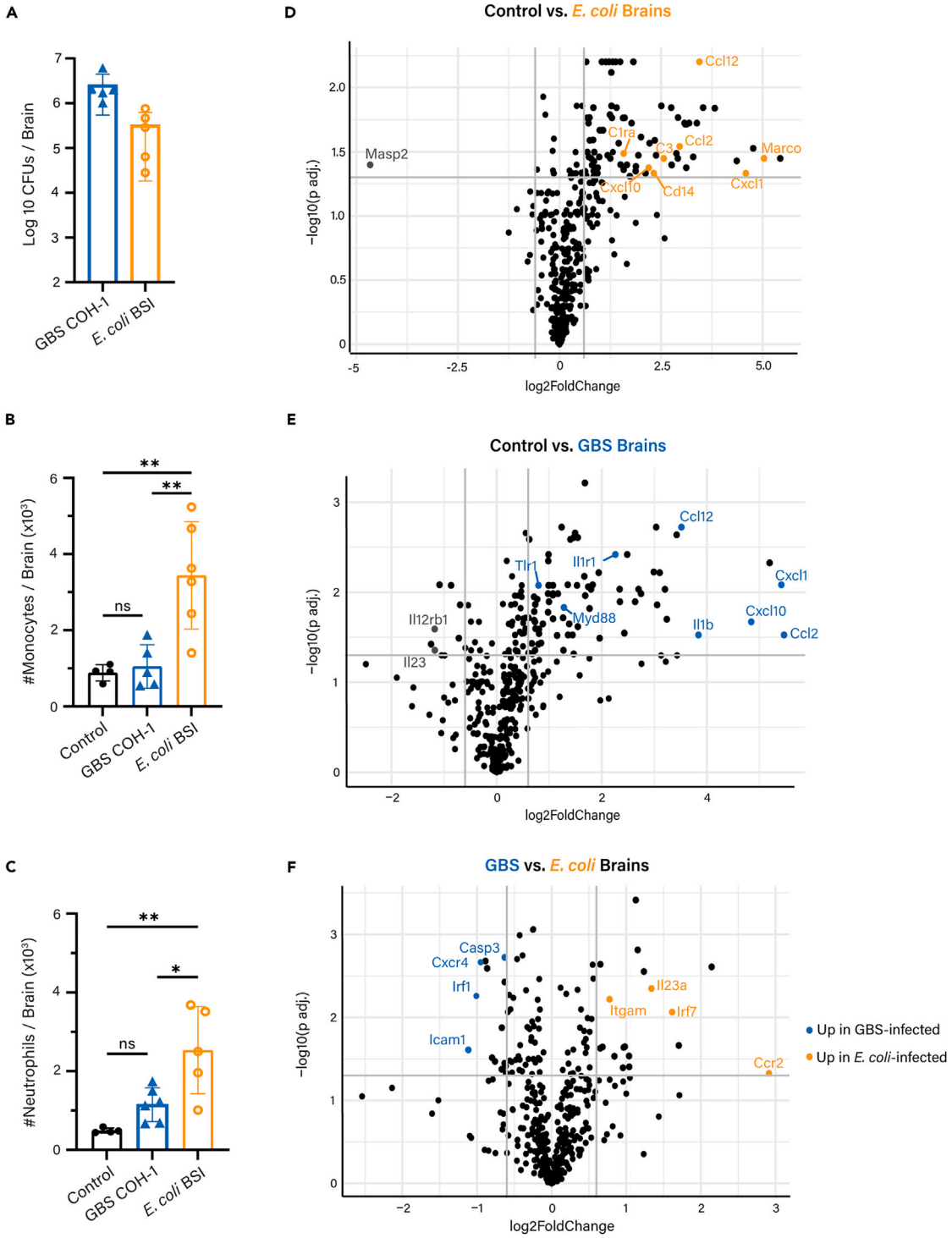

Figure 4. Neuroinflammation is a feature of *E. coli* and GBS neonatal sepsis

BL/6 P7 pups were infected with GBS or *E. coli* on P7.

(A) GBS and *E. coli* CFUs from the perfused brains of *E. coli*-infected or GBS-infected pups 18 h post-infection.

Figure 4. *Continued*

(B) Absolute number of monocytes (CD45hi, CD11b+, Ly6C+, Ly6Glow) and (C) Neutrophils (CD45hi, CD11b+, Ly6Clow, Ly6G+) in the perfused brains of *E. coli*-infected or GBS-infected 18 h post-infection.

(D) Volcano plot of differentially expressed genes between BL/6 uninfected control vs. *E. coli* infected P7 pups, (E) Volcano plot of differentially expressed genes between BL/6 uninfected control vs. GBS infected P7 pups, and (F) Volcano plot of differentially expressed genes between GBS-infected vs. *E. coli*-infected P7 pups. Data shown is from four independent experiments, $n > 4$ mice per group. Controls are uninfected age-matched littermates. Statistical tests used include one-way ANOVA (B, C) with ns = $p > 0.05$, * = $p \leq 0.05$, ** = $p \leq 0.01$.

E. coli, but not GBS-infected pups (Figure 5A). Importantly, the majority of these Nur77+ CD69$^+$ γδ T cells also expressed CCR6 (Figure 5B), demonstrating that in the brain, IL-17 producing γδ T cells undergo TCR-mediated activation during neonatal *E. coli* sepsis.

To determine the contribution of γδ T cells to GBS and *E. coli* sepsis-associated neuroinflammation, we compared immunological gene expression between BL/6 and TCRδ−/− pups. TCRδ−/− pups were used to evaluate the contribution of γδ T cells to sepsis-induced neuroinflammation, as treatment with the anti-TCRγδ UC7-13D5 antibody did not affect brain-resident γδ T cells (Figure S3B). While there were significant differences in gene expression between uninfected BL/6 and TCRδ−/− pups (Figure S6B), these conditions clustered similarly to one another, and distinctly from the infection points (Figure S6A). Analysis of the brain by Nanostring revealed fifty-eight differentially expressed genes between BL/6 and TCRδ−/− *E. coli*-infected pups. Compared to BL/6 *E coli*-infected pups, TCRδ−/− *E. coli*-infected pups had increased expression of genes associated with apoptosis, such as *Casp-3*, *Psmb5* and *Mapk1* (Figure 5C). Notably, uninfected TCRδ−/− pups also had increased *Casp-3* expression compared to uninfected wildtype (WT) BL/6 mice (Figure S6B), suggesting that γδ T cells may protect the neonatal brain from apoptosis both at baseline and during systemic inflammation. Compared to TCRδ−/− *E. coli*-infected pups, WT BL/6 *E. coli*-infected pups had increased expression of *Il23a*, *Il12rb1*, and *Stat5b* (Figure 5C). *Il23a and Il12rb1* were also increased in uninfected WT BL/6 pups compared to TCRδ−/− pups, suggesting a role for γδ T cells in driving IL12/IL23 cytokine signaling at baseline and during *E. coli*-mediated systemic inflammation.

During GBS infection, there were twenty-two differentially expressed genes between BL/6 and TCRδ−/− GBS-infected pups. Compared to TCRδ−/− GBS-infected pups, BL/6 pups had increased expression of *H2-Dmb2*, along with *Tgfbr1*, *Il6ra*, and *Smad5* (Figure 5D), suggesting a role for γδ T cells in antigen presentation and TGF-β signaling, respectively. Moreover, PCA also revealed distinct clustering of TCRδ−/− *E. coli*-infected pups and TCRδ−/− GBS-infected pups (Figure S6A). Taken together, these data suggest that γδ T cells play an infection-specific role during sepsis-associated neuroinflammation.

DISCUSSION

The present study reveals that γδ T cells undergo rapid activation and cytokine production during a murine model of single-organism *Streptococcus agalactiae* (GBS) and *Escherichia coli* neonatal sepsis (Figure 1), and that GBS and *E. coli* septicemia induce activation of IFN-γ and IL-17 producing γδ T cells, respectively (Figure 2). Notably, a greater proportion and absolute number of γδ T cells were activated in response to *E. coli* infection compared to GBS infection (Figures 1A–1C), despite higher pathogen burden during GBS infection (Figures 3F and S3C). These findings may suggest that bacterial components, rather than bacterial burden alone, are critical in driving the magnitude of the neonatal γδ T cell response. Therefore, how components of *E. coli* and GBS drive differential γδ T cell activation will be the subject of continued investigation.

Although the γδ T cell compartment had the highest proportion of cells undergoing activation in response to both *E. coli* and GBS infections, a modest increase in activation status was observed for CD4$^+$ and CD8$^+$ T cells, and B cells (Figures S1A–S1C). This small proportion of activated CD8$^+$ T cells may represent "virtual memory" (T_{VM}) T cells, which are abundant in neonates.[42,43] Increased activation status of CD8$^+$ T cells at the early time point of 18 h post-infection may further implicate T_{VM} cells, as they are capable of responding to infection faster than naive T cells due to their memory-like capacity.[44,45]

An additional outstanding question raised by the present findings is the extent to which γδ T cell effector cytokine responses depend directly on bacterial factors such as virulence factors vs. the upstream immune response to such bacterial components. The clinical isolate of *E. coli* used herein is an extraintestinal pathogenic *E. coli* (ExPEC) that expresses several virulence genes, including the capsular polysaccharide K1.[3,7] The K1 antigen has been implicated in various neonatal infections, including meningitis and sepsis,[46] and plays a critical role in the ability of *E. coli* to resist phagocytosis and invade the central nervous system.[47] Similarly, GBS COH-1 (ATCC) is a highly virulent, encapsulated serotype III clinical isolate that expresses virulence factors involved in immune resistance and neuroinvasion, including the serine protease CspA,[48] and invasion-associated gene (IagA),[49] respectively. Thus, the extent to which activation and cytokine production from γδ T cells is dependent on bacterial virulence factors vs. signals from the inflammatory milleu requires further investigation. We also report that γδ T cells undergo distinct pathways of activation to elicit their effector cytokine responses during *E. coli* and GBS sepsis. During GBS infection, there was no change in the proportion of CD69$^+$ Nur77+ γδ T cells in the spleen or brain (Figures 3A, 3B, and 5A), suggesting TCR-independent γδ T cell activation and IFN-γ production. As γδTCR signaling was not implicated during GBS infection, the use of the γδTCR blocking antibody during GBS infection conferred no survival benefit or change in pathogen burden (Figures S3C and S3D). Similar to Natural Killer (NK) cells, γδ T cells can produce IFN-γ in response to IL-12, and IL-18,[34,50] and upon engagement of NKG2D ligands by host stress molecules.[51] Analysis of the serum from GBS-infected pups revealed no statistically significant increase in IL-12 or IL-18 production (Figures S4A–S4C), suggesting that other host stress factors are driving IFN-γ production. Furthermore, the exact mechanism by which CD27$^+$ γδ T cells become activated and make IFN-γ during GBS sepsis will be the subject of future studies.

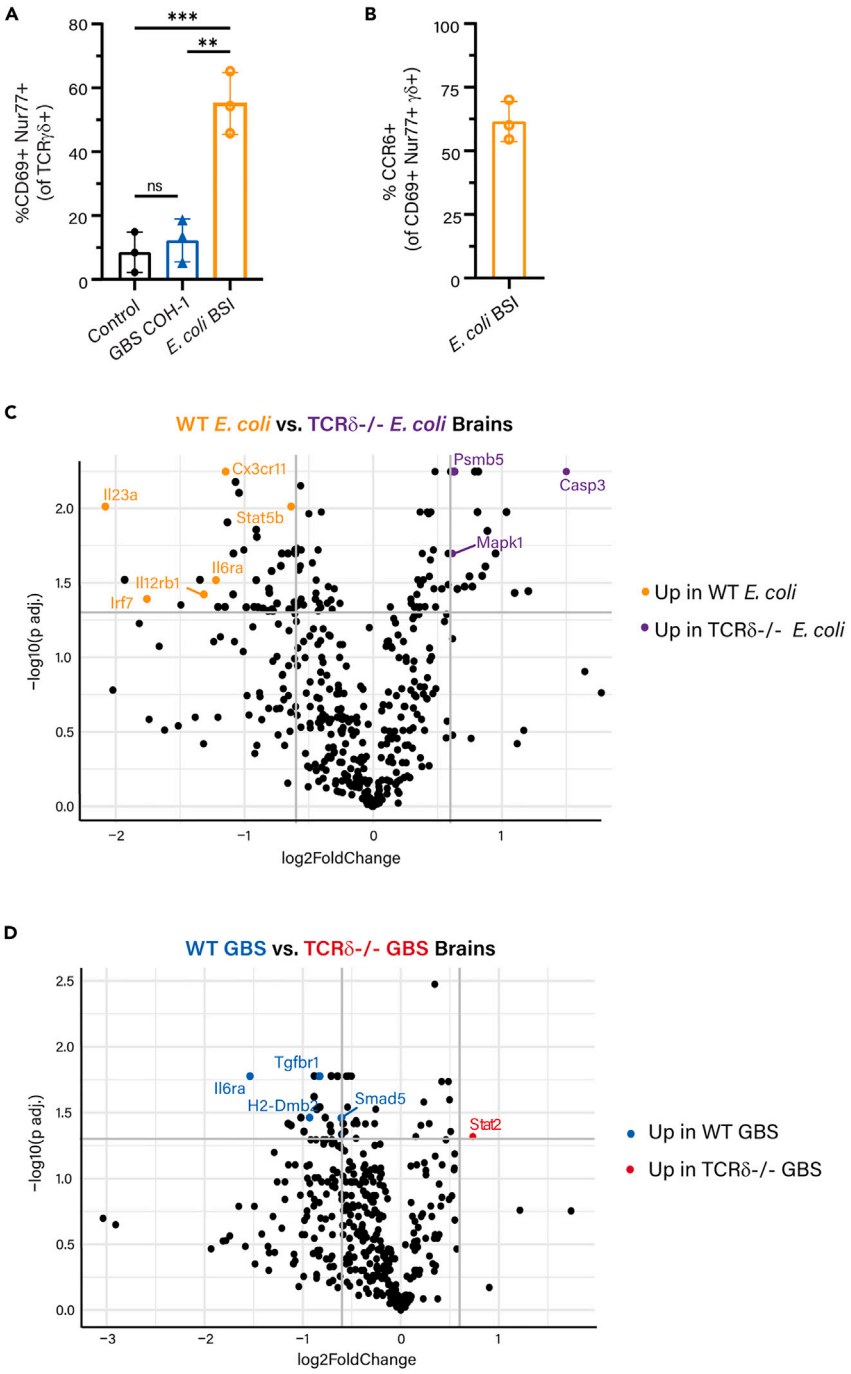

Figure 5. γδ+ T cells differentially impact GBS and *E. coli*-driven neuroinflammation

Nur77GFP pups were infected with GBS, or *E. coli* on P7, and brains were harvested 18 h post-infection.

(A) Proportion of Nur77+ CD69^{+} γδ+ T cells in the perfused brain of GBS-infected or *E. coli*-infected Nur77-GFP P7 pups.

(B) CCR6 expression of Nur77+ CD69^{+} γδ+ T cells in the spleen and brain of *E. coli*-infected pups.

(C and D) TCRδ−/− pups were infected with GBS or *E. coli* on P7, and brains were harvested 18 h post-infection. Volcano plots of differentially expressed genes in the brains of C) *E. coli* infected, or D) GBS-infected BL/6 vs. TCRδ−/− pups. Controls are uninfected age-matched littermates. Data shown is from three independent experiments, $n > 3$ mice per group. Statistics used include one-way ANOVA (A) with ns = $p > 0.05$, ** = $p \leq 0.01$, *** = $p \leq 0.001$.

Conversely, during *E. coli* sepsis, there was a robust increase in the proportion of Nur77+ CD69^{+} γδ T cells in both the spleen and brain (Figures 3B and 5A), suggesting that γδ T cells undergo TCR-mediated activation during *E. coli* sepsis. We also report that splenocyte co-culture with HK *E. coli* was sufficient to induce Nur77 expression in neonatal γδ T cells (Figure S2), however, the nature of the antigen driving γδ TCR-mediated activation remains unknown. Thus, whether splenic γδ T cells are directly recognizing a heat-stable *E. coli* bacterial product or a host stress molecule that is upregulated in response to both live and HK bacteria, will be the subject of future studies.

Interestingly, we also find that γδTCR signaling during *E. coli* neonatal sepsis is pathogenic, as blocking the γδTCR with the UC7-13D5 antibody was sufficient to rescue mortality (Figures 3E and S3A). γδTCR signaling during *E. coli* infection was further associated with the production of IL-17, as a majority of the TCR-activated γδ T cells in the spleen and brain expressed CCR6 (Figures 3C and 5B). Moreover, blockade of the γδTCR during *E. coli* infection was sufficient to ablate the IL-17 serum signature seen in isotype-treated pups (Figure 3D). Improved survival of *E. coli*-infected pups upon blockade of the γδTCR may be due to the reduced production of IL-17 (Figures 3D and 3E), as IL-17 has been shown to drive mortality in other models of neonatal sepsis.[52] Intriguingly, the complete rescue of mortality upon the blockade of γδ T cell functions contrasts with other early-life infections in which γδ T cells are protective to the neonate, including neonatal influenza[23] and *Clostridium difficile* infection.[24] The conflicting role of γδ T cells as pathogenic during *E. coli* sepsis vs. protective during other neonatal infections could be due to the state of immune dysregulation and hyperinflammation that occurs during sepsis, however, the exact nature of these signals, and their specific impact on γδ T cell function, remain unknown. Additionally, these findings raise important questions surrounding the impact of systemic vs. local, tissue-specific γδ T cell responses, and whether a pathogenic contribution of γδ T cells is more likely during a systemic infection.

γδTCR signaling from IL-17+ γδ T cells in the spleen and brain during *E. coli* sepsis also raises interesting questions surrounding γδ T cell subsets and TCR specificity across different organs. γδ T cells develop in discrete sequential waves based on the usage of γ and δ chain pairings, which determine both their effector function and tissue-homing properties.[18] The γδTCR repertoire and V(D)J diversity vary across subsets, with CNS-resident IL-17+ γδ T cells primarily expressing the invariant Vγ6 chain, and IL-17+ γδ T cells residing outside of the CNS expressing either the Vγ1, Vγ4, or Vγ6 chain, which display varying levels of V(D)J diversity.[29] Therefore, although there was an increase in the proportion of Nur77+ CD69^{+} γδ T cells in both the spleen and brain, which subset of IL-17+ γδ T cell is responding to *E. coli* infection in these tissues, along with the nature of the antigen they recognize, remain unknown. Furthermore, whether the γδ T cells in the CNS and periphery recognize the same antigen despite varying TCR repertoire and diversity across these tissues is an interesting direction for future study. Therefore, future analysis will aim to better define the *E. coli* pathogen or host-derived antigen(s) recognized by the γδTCR, along with the contribution of γδ T cell subsets to the unique inflammatory environment in septic tissues.

Post-infectious neurological sequelae represent a significant co-morbidity in survivors of neonatal sepsis.[35] The present study therefore sought to characterize the unique neuroinflammatory signatures associated with GBS and *E. coli* systemic infection, and the extent to which these signatures are dependent upon γδ T cells. Significant bacterial burden was found in the perfused brains of both GBS and *E. coli*-infected pups (Figure 4A), demonstrating the capacity of both GBS COH-1 and *E. coli* BSI-B for neuroinvasion. Interestingly, *E. coli* infection induced greater infiltration of monocytes and neutrophils in the brain (Figures 4B and 4C), despite both GBS and *E. coli* showing increased gene expression of potent monocyte and neutrophil chemotactic factors, such as *Ccl2*, *Cxcl1*, and *Cxcl10*, respectively (Figures 4D and 4E). Differences in neutrophil and monocyte infiltration into the brain during GBS infection may be due to the increased expression of *Casp-3* in the brains of GBS-infected pups compared to *E. coli*-infected pups (Figure 4F). Furthermore, increased cell death could contribute to the lack of live cellular infiltrate into the brain during GBS infection, as only live cells are used for quantification (Figure S5). Thus, live monocytes and neutrophils may be recruited to the neonatal brain during GBS infection, but may be undergoing apoptosis due to signals in the inflammatory environment. Similarly, which cell type expresses *Casp-3* during GBS infection, and whether this expression is protective or pathogenic, represents an important direction for future study. Furthermore, during *E. coli* sepsis, and at baseline, there was increased *Casp-3* expression in the brains of TCRδ−/− pups compared to BL/6 infected pups, suggesting that γδ T cells in the brain at homeostasis, and during *E. coli* infection may suppress apoptosis (Figures 5C and S6B). Whether this anti-apoptotic effect is due to the direct action of γδ T cell-derived IL-17 was not addressed herein, although IL-17 has been shown to have a pro-survival effect on tumor cells,[53] and B cells,[54] however, its exact role in this context remains unknown.

Compared to *E. coli* infection, there were fewer differentially expressed genes between BL/6 and TCRδ−/− pups infected with GBS (Figures 5C and 5D), which may suggest a more minor role for γδ T cells during GBS compared to *E. coli* neuroinflammation. In the absence of γδ T cells during neonatal GBS infection, there was decreased expression of genes involved in MHC II antigen presentation, including *H2-Dmb2*, which facilitates the removal of Class II-associated invariant chain peptide (CLIP) from MHC II molecules.[55,56] Similarly, *Il6ra*, *Tgfbr1*, and *Smad3* were also increased in the BL/6 compared to TCRδ−/− GBS infected pups, suggesting that during GBS infection, γδ T cells may impact TGF-β signaling (Figure 5D). Furthermore, mechanisms by which γδ T cells influence MHCII antigen presentation and TGF-β signaling, and how these pathways impact neurological outcomes in septic neonatal mice, represents an important direction for future study. Moreover, future studies utilizing proteomics or single-cell RNA sequencing may help elucidate differential pathways upregulated by γδ T cells in the periphery and brain during *E. coli* and GBS neonatal sepsis.

These data present evidence that γδ T cell responses during neonatal sepsis rely heavily on the initiating pathogen. The finding that context-specific γδ T cell responses differentially impact mortality may have important clinical implications for the treatment of neonatal sepsis. Overall, this work will help elucidate the pathogen-specific contributions of neonatal γδ T cells to sepsis-induced immunopathology and neuroinflammation.

Limitations of the study

One significant limitation of the present study is the use of TCRδ−/− pups for survival analysis. During *E. coli* infection, neutralization of the γδTCR was sufficient to rescue mortality, however, TCRδ−/− pups succumbed to *E. coli*-induced mortality at a similar rate as WT pups

(Figure 3E). As γδTCR signaling is also absent in TCRδ−/− pups, the lack of improved survival in TCRδ−/− pups may suggest a physiological perturbation from a developmental deficiency of γδ T cells.[18] Additionally, whether there are TCR-independent contributions from γδ T cells during *E. coli* infection remains unclear. WT and TCRδ−/− mice also succumbed to GBS infection at similar rates (Figure S3D). Thus, whether γδ T cells are pathogenic during GBS infection, or if the lack of improved survival in TCRδ−/− is due to physiologic changes resulting from a lack of γδ T cells, is not robustly addressed herein. Future studies will utilize inducible deletion of the γδ T cell compartment to ameliorate off-target effects of global γδ T cell deletion.

STAR★METHODS

Detailed methods are provided in the online version of this paper and include the following:

- KEY RESOURCES TABLE
- RESOURCE AVAILABILITY
  - Lead contact
  - Materials availability
  - Data and code availability
- EXPERIMENTAL MODEL AND STUDY PARTICIPANT DETAILS
  - Mice
- METHOD DETAILS
  - Preparation of bacteria
  - Enzyme-Linked Immunosorbent Assay (ELISA)
  - Flow cytometry
  - Liver digestion for analysis by flow cytometry
  - Intracellular cytokine staining
  - Brain isolation for analysis by flow cytometry
  - mRNA isolation from brains
  - Nanostring
- QUANTIFICATION AND STATISTICAL ANALYSIS

SUPPLEMENTAL INFORMATION

Supplemental information can be found online at https://doi.org/10.1016/j.isci.2024.109669.

ACKNOWLEDGMENTS

This study was supported by funding from the NIH: T32 AI170478 (L.T.W.), and R01 DK134366 (K.A.K.).

AUTHOR CONTRIBUTIONS

Conceptualization, L.T.W. and K.A.K.; methodology, L.T.W., K.G.G. and K.A.K; investigation, L.T.W., K.G.G., and K.A.K; writing – original draft, L.T.W. and K.A.K.; writing – review & editing, L.T.W. and K.A.K.; funding acquisition, L.T.W. and K.A.K.; resources, L.T.W. and K.A.K.

DECLARATION OF INTERESTS

The authors declare no competing interests.

Received: October 12, 2023
Revised: January 22, 2024
Accepted: April 2, 2024
Published: April 5, 2024

REFERENCES

1. Bergin, S.P., Thaden, J.T., Ericson, J.E., Cross, H., Messina, J., Clark, R.H., Fowler, V.G., Jr., Benjamin, D.K., Jr., Hornik, C.P., and Smith, P.B.; Antibacterial Resistance Leadership Group (2015). Neonatal Escherichia coli Bloodstream Infections: Clinical Outcomes and Impact of Initial Antibiotic Therapy. Pediatr. Infect. Dis. J. *34*, 933–936. https://doi.org/10.1097/inf.0000000000000769.
2. Stoll, B.J., Hansen, N.I., Sánchez, P.J., Faix, R.G., Poindexter, B.B., Van Meurs, K.P., Bizzarro, M.J., Goldberg, R.N., Frantz, I.D., 3rd, Hale, E.C., et al. (2011). Early onset neonatal sepsis: the burden of group B Streptococcal and E. coli disease continues. Pediatrics *127*, 817–826. https://doi.org/10.1542/peds.2010-2217.
3. Knoop, K.A., Coughlin, P.E., Floyd, A.N., Ndao, I.M., Hall-Moore, C., Shaikh, N., Gasparrini, A.J., Rusconi, B., Escobedo, M., Good, M., et al. (2020). Maternal activation of the EGFR prevents translocation of gut-residing pathogenic Escherichia coli in a model of late-onset neonatal sepsis. Proc. Natl. Acad. Sci. USA *117*, 7941–7949. https://doi.org/10.1073/pnas.1912022117.
4. Segura-Cervantes, E., Mancilla-Ramírez, J., González-Canudas, J., Alba, E., Santillán-Ballesteros, R., Morales-Barquet, D., Sandoval-Plata, G., and Galindo-Sevilla, N. (2016). Inflammatory Response in Preterm and Very Preterm Newborns with Sepsis.

Mediat. Inflamm. *2016*, 6740827. https://doi.org/10.1155/2016/6740827.
5. Shane, A.L., Sánchez, P.J., and Stoll, B.J. (2017). Neonatal sepsis. Lancet *390*, 1770–1780. https://doi.org/10.1016/S0140-6736(17)31002-4.
6. Basu, S. (2015). Neonatal sepsis: the gut connection. Eur. J. Clin. Microbiol. Infect. Dis. *34*, 215–222. https://doi.org/10.1007/s10096-014-2232-6.
7. Carl, M.A., Ndao, I.M., Springman, A.C., Manning, S.D., Johnson, J.R., Johnston, B.D., Burnham, C.A.D., Weinstock, E.S., Weinstock, G.M., Wylie, T.N., et al. (2014). Sepsis from the gut: the enteric habitat of bacteria that cause late-onset neonatal bloodstream infections. Clin. Infect. Dis. *58*, 1211–1218. https://doi.org/10.1093/cid/ciu084.
8. Heath, P.T., and Jardine, L.A. (2014). Neonatal infections: group B streptococcus. Clin. Evid. *2014*, 0323.
9. Mynarek, M., Bjellmo, S., Lydersen, S., Afset, J.E., Andersen, G.L., and Vik, T. (2021). Incidence of invasive Group B Streptococcal infection and the risk of infant death and cerebral palsy: a Norwegian Cohort Study. Pediatr. Res. *89*, 1541–1548. https://doi.org/10.1038/s41390-020-1092-2.
10. Tavares, T., Pinho, L., and Bonifácio Andrade, E. (2022). Group B Streptococcal Neonatal Meningitis. Clin. Microbiol. Rev. *35*, e0007921. https://doi.org/10.1128/cmr.00079-21.
11. Tsafaras, G.P., Ntontsi, P., and Xanthou, G. (2020). Advantages and Limitations of the Neonatal Immune System. Front. Pediatr. *8*, 5. https://doi.org/10.3389/fped.2020.00005.
12. Barrios, C., Brawand, P., Berney, M., Brandt, C., Lambert, P.H., and Siegrist, C.A. (1996). Neonatal and early life immune responses to various forms of vaccine antigens qualitatively differ from adult responses: predominance of a Th2-biased pattern which persists after adult boosting. Eur. J. Immunol. *26*, 1489–1496. https://doi.org/10.1002/eji.1830260713.
13. Basha, S., Surendran, N., and Pichichero, M. (2014). Immune responses in neonates. Expet Rev. Clin. Immunol. *10*, 1171–1184. https://doi.org/10.1586/1744666x.2014.942288.
14. Li, L., Lee, H.H., Bell, J.J., Gregg, R.K., Ellis, J.S., Gessner, A., and Zaghouani, H. (2004). IL-4 utilizes an alternative receptor to drive apoptosis of Th1 cells and skews neonatal immunity toward Th2. Immunity *20*, 429–440. https://doi.org/10.1016/s1074-7613(04)00072-x.
15. Semmes, E.C., Chen, J.-L., Goswami, R., Burt, T.D., Permar, S.R., and Fouda, G.G. (2020). Understanding Early-Life Adaptive Immunity to Guide Interventions for Pediatric Health. Front. Immunol. *11*, 595297. https://doi.org/10.3389/fimmu.2020.595297.
16. Chien, Y.H., Meyer, C., and Bonneville, M. (2014). γδ T cells: first line of defense and beyond. Annu. Rev. Immunol. *32*, 121–155. https://doi.org/10.1146/annurev-immunol-032713-120216.
17. Vantourout, P., and Hayday, A. (2013). Six-of-the-best: unique contributions of γδ T cells to immunology. Nat. Rev. Immunol. *13*, 88–100. https://doi.org/10.1038/nri3384.
18. Ribot, J.C., Lopes, N., and Silva-Santos, B. (2021). γδ T cells in tissue physiology and surveillance. Nat. Rev. Immunol. *21*, 221–232. https://doi.org/10.1038/s41577-020-00452-4.
19. Havran, W.L., and Allison, J.P. (1988). Developmentally ordered appearance of thymocytes expressing different T-cell antigen receptors. Nature *335*, 443–445. https://doi.org/10.1038/335443a0.
20. Parker, M.E., and Ciofani, M. (2020). Regulation of γδ T Cell Effector Diversification in the Thymus. Front. Immunol. *11*, 42. https://doi.org/10.3389/fimmu.2020.00042.
21. Dimova, T., Brouwer, M., Gosselin, F., Tassignon, J., Leo, O., Donner, C., Marchant, A., and Vermijlen, D. (2015). Effector Vγ9Vδ2 T cells dominate the human fetal γδ T-cell repertoire. Proc. Natl. Acad. Sci. USA *112*, E556–E565. https://doi.org/10.1073/pnas.1412058112.
22. Gibbons, D.L., Haque, S.F.Y., Silberzahn, T., Hamilton, K., Langford, C., Ellis, P., Carr, R., and Hayday, A.C. (2009). Neonates harbour highly active gammadelta T cells with selective impairments in preterm infants. Eur. J. Immunol. *39*, 1794–1806. https://doi.org/10.1002/eji.200939222.
23. Guo, X.Z.J., Dash, P., Crawford, J.C., Allen, E.K., Zamora, A.E., Boyd, D.F., Duan, S., Bajracharya, R., Awad, W.A., Apiwattanakul, N., et al. (2018). Lung γδ T Cells Mediate Protective Responses during Neonatal Influenza Infection that Are Associated with Type 2 Immunity. Immunity *49*, 531–544.e6. https://doi.org/10.1016/j.immuni.2018.07.011.
24. Chen, Y.S., Chen, I.B., Pham, G., Shao, T.Y., Bangar, H., Way, S.S., and Haslam, D.B. (2020). IL-17-producing γδ T cells protect against Clostridium difficile infection. J. Clin. Invest. *130*, 2377–2390. https://doi.org/10.1172/jci127242.
25. Scasso, S., Laufer, J., Rodriguez, G., Alonso, J.G., and Sosa, C.G. (2015). Vaginal group B streptococcus status during intrapartum antibiotic prophylaxis. Int. J. Gynaecol. Obstet. *129*, 9–12. https://doi.org/10.1016/j.ijgo.2014.10.018.
26. Yadeta, T.A., Worku, A., Egata, G., Seyoum, B., Marami, D., and Berhane, Y. (2018). Vertical transmission of group B Streptococcus and associated factors among pregnant women: a cross-sectional study, Eastern Ethiopia. Infect. Drug Resist. *11*, 397–404. https://doi.org/10.2147/idr.S150029.
27. Travier, L., Alonso, M., Andronico, A., Hafner, L., Disson, O., Lledo, P.M., Cauchemez, S., and Lecuit, M. (2021). Neonatal susceptibility to meningitis results from the immaturity of epithelial barriers and gut microbiota. Cell Rep. *35*, 109319. https://doi.org/10.1016/j.celrep.2021.109319.
28. Haas, J.D., González, F.H.M., Schmitz, S., Chennupati, V., Föhse, L., Kremmer, E., Förster, R., and Prinz, I. (2009). CCR6 and NK1.1 distinguish between IL-17A and IFN-gamma-producing gammadelta effector T cells. Eur. J. Immunol. *39*, 3488–3497. https://doi.org/10.1002/eji.200939922.
29. Muñoz-Ruiz, M., Sumaria, N., Pennington, D.J., and Silva-Santos, B. (2017). Thymic Determinants of γδ T Cell Differentiation. Trends Immunol. *38*, 336–344. https://doi.org/10.1016/j.it.2017.01.007.
30. Constant, P., Davodeau, F., Peyrat, M.A., Poquet, Y., Puzo, G., Bonneville, M., and Fournié, J.J. (1994). Stimulation of human gamma delta T cells by nonpeptidic mycobacterial ligands. Science *264*, 267–270. https://doi.org/10.1126/science.8146660.
31. Ashouri, J.F., and Weiss, A. (2017). Endogenous Nur77 Is a Specific Indicator of Antigen Receptor Signaling in Human T and B Cells. J. Immunol. *198*, 657–668. https://doi.org/10.4049/jimmunol.1601301.
32. Moran, A.E., Holzapfel, K.L., Xing, Y., Cunningham, N.R., Maltzman, J.S., Punt, J., and Hogquist, K.A. (2011). T cell receptor signal strength in Treg and iNKT cell development demonstrated by a novel fluorescent reporter mouse. J. Exp. Med. *208*, 1279–1289. https://doi.org/10.1084/jem.20110308.
33. Koenecke, C., Chennupati, V., Schmitz, S., Malissen, B., Förster, R., and Prinz, I. (2009). In vivo application of mAb directed against the gammadelta TCR does not deplete but generates "invisible" gammadelta T cells. Eur. J. Immunol. *39*, 372–379. https://doi.org/10.1002/eji.200838741.
34. Silva-Santos, B., Mensurado, S., and Coffelt, S.B. (2019). γδ T cells: pleiotropic immune effectors with therapeutic potential in cancer. Nat. Rev. Cancer *19*, 392–404. https://doi.org/10.1038/s41568-019-0153-5.
35. Stoll, B.J., Hansen, N.I., Adams-Chapman, I., Fanaroff, A.A., Hintz, S.R., Vohr, B., and Higgins, R.D.; National Institute of Child Health and Human Development Neonatal Research Network (2004). Neurodevelopmental and Growth Impairment Among Extremely Low-Birth-Weight Infants With Neonatal Infection. JAMA *292*, 2357–2365. https://doi.org/10.1001/jama.292.19.2357.
36. Ribeiro, M., Brigas, H.C., Temido-Ferreira, M., Pousinha, P.A., Regen, T., Santa, C., Coelho, J.E., Marques-Morgado, I., Valente, C.A., Omenetti, S., et al. (2019). Meningeal γδ T cell-derived IL-17 controls synaptic plasticity and short-term memory. Sci. Immunol. *4*, eaay5199. https://doi.org/10.1126/sciimmunol.aay5199.
37. Wo, J., Zhang, F., Li, Z., Sun, C., Zhang, W., and Sun, G. (2020). The Role of Gamma-Delta T Cells in Diseases of the Central Nervous System. Front. Immunol. *11*, 580304. https://doi.org/10.3389/fimmu.2020.580304.
38. Park, J.H., Kang, I., and Lee, H.K. (2022). γδ T Cells in Brain Homeostasis and Diseases. Front. Immunol. *13*, 886397. https://doi.org/10.3389/fimmu.2022.886397.
39. Gentles, A.J., Newman, A.M., Liu, C.L., Bratman, S.V., Feng, W., Kim, D., Nair, V.S., Xu, Y., Khuong, A., Hoang, C.D., et al. (2015). The prognostic landscape of genes and infiltrating immune cells across human cancers. Nat. Med. *21*, 938–945. https://doi.org/10.1038/nm.3909.
40. Gelderblom, M., Arunachalam, P., and Magnus, T. (2014). γδ T cells as early sensors of tissue damage and mediators of secondary neurodegeneration. Front. Cell. Neurosci. *8*, 368. https://doi.org/10.3389/fncel.2014.00368.
41. Welte, T., Lamb, J., Anderson, J.F., Born, W.K., O'Brien, R.L., and Wang, T. (2008). Role of two distinct gammadelta T cell subsets during West Nile virus infection. FEMS Immunol. Med. Microbiol. *53*, 275–283. https://doi.org/10.1111/j.1574-695X.2008.00430.x.
42. Akue, A.D., Lee, J.Y., and Jameson, S.C. (2012). Derivation and maintenance of virtual memory CD8 T cells. J. Immunol. *188*, 2516–2523. https://doi.org/10.4049/jimmunol.1102213.
43. Schüler, T., Hämmerling, G.J., and Arnold, B. (2004). Cutting edge: IL-7-dependent homeostatic proliferation of CD8+ T cells in neonatal mice allows the generation of long-lived natural memory T cells. J. Immunol. *172*,

15–19. https://doi.org/10.4049/jimmunol.172.1.15.

44. Haluszczak, C., Akue, A.D., Hamilton, S.E., Johnson, L.D.S., Pujanauski, L., Teodorovic, L., Jameson, S.C., and Kedl, R.M. (2009). The antigen-specific CD8+ T cell repertoire in unimmunized mice includes memory phenotype cells bearing markers of homeostatic expansion. J. Exp. Med. *206*, 435–448. https://doi.org/10.1084/jem.20081829.
45. Lee, J.-Y., Hamilton, S.E., Akue, A.D., Hogquist, K.A., and Jameson, S.C. (2013). Virtual memory CD8 T cells display unique functional properties. Proc. Natl. Acad. Sci. USA *110*, 13498–13503. https://doi.org/10.1073/pnas.1307572110.
46. Kaczmarek, A., Budzyńska, A., and Gospodarek, E. (2014). Detection of K1 antigen of Escherichia coli rods isolated from pregnant women and neonates. Folia Microbiol. *59*, 419–422. https://doi.org/10.1007/s12223-014-0315-5.
47. Hoffman, J.A., Wass, C., Stins, M.F., and Kim, K.S. (1999). The capsule supports survival but not traversal of Escherichia coli K1 across the blood-brain barrier. Infect. Immun. *67*, 3566–3570. https://doi.org/10.1128/iai.67.7.3566-3570.1999.
48. Harris, T.O., Shelver, D.W., Bohnsack, J.F., and Rubens, C.E. (2003). A novel streptococcal surface protease promotes virulence, resistance to opsonophagocytosis, and cleavage of human fibrinogen. J. Clin. Invest. *111*, 61–70. https://doi.org/10.1172/jci16270.
49. Doran, K.S., Engelson, E.J., Khosravi, A., Maisey, H.C., Fedtke, I., Equils, O., Michelsen, K.S., Arditi, M., Peschel, A., and Nizet, V. (2005). Blood-brain barrier invasion by group B Streptococcus depends upon proper cell-surface anchoring of lipoteichoic acid. J. Clin. Invest. *115*, 2499–2507. https://doi.org/10.1172/jci23829.
50. Sedlak, C., Patzl, M., Saalmüller, A., and Gerner, W. (2014). IL-12 and IL-18 induce interferon-γ production and *de novo* CD2 expression in porcine γδ T cells. Dev. Comp. Immunol. *47*, 115–122. https://doi.org/10.1016/j.dci.2014.07.007.
51. Rincon-Orozco, B., Kunzmann, V., Wrobel, P., Kabelitz, D., Steinle, A., and Herrmann, T. (2005). Activation of V gamma 9V delta 2 T cells by NKG2D. J. Immunol. *175*, 2144–2151. https://doi.org/10.4049/jimmunol.175.4.2144.
52. Wynn, J.L., Wilson, C.S., Hawiger, J., Scumpia, P.O., Marshall, A.F., Liu, J.-H., Zharkikh, I., Wong, H.R., Lahni, P., Benjamin, J.T., et al. (2016). Targeting IL-17A attenuates neonatal sepsis mortality induced by IL-18. Proc. Natl. Acad. Sci. USA *113*, E2627.
53. Nam, J.S., Terabe, M., Kang, M.J., Chae, H., Voong, N., Yang, Y.A., Laurence, A., Michalowska, A., Mamura, M., Lonning, S., et al. (2008). Transforming growth factor beta subverts the immune system into directly promoting tumor growth through interleukin-17. Cancer Res. *68*, 3915–3923. https://doi.org/10.1158/0008-5472.Can-08-0206.
54. Xu, S., and Cao, X. (2010). Interleukin-17 and its expanding biological functions. Cell. Mol. Immunol. *7*, 164–174. https://doi.org/10.1038/cmi.2010.21.
55. Doebele, R.C., Busch, R., Scott, H.M., Pashine, A., and Mellins, E.D. (2000). Determination of the HLA-DM interaction site on HLA-DR molecules. Immunity *13*, 517–527. https://doi.org/10.1016/s1074-7613(00)00051-0.
56. Santambrogio, L., Berendam, S.J., and Engelhard, V.H. (2019). The Antigen Processing and Presentation Machinery in Lymphatic Endothelial Cells. Front. Immunol. *10*, 1033. https://doi.org/10.3389/fimmu.2019.01033.
57. Cumba Garcia, L.M., Huseby Kelcher, A.M., Malo, C.S., and Johnson, A.J. (2016). Superior isolation of antigen-specific brain infiltrating T cells using manual homogenization technique. J. Immunol. Methods *439*, 23–28. https://doi.org/10.1016/j.jim.2016.09.002.

STAR★METHODS

KEY RESOURCES TABLE

REAGENT or RESOURCE	SOURCE	IDENTIFIER
Antibodies		
PE/Cy7-labeled CD45 (clone: 30-F11)	Biolegend	103114; RRID:AB_312979
BV605-labeled CD45 (clone: 30-F11)	Biolegend	103139; RRID:AB_2562341
BV421-labeled CD4 (clone: GK1.5)	Biolegend	100443: RRID:AB_1120371
BV510-labeled CD8 (clone: 53-6.7)	Biolegend	100751; RRID:AB_2563057
BV510-labeled CD11b (clone: M1/70)	Biolegend	101245; RRID:AB_2561390
BV421-labeled TCRγδ (clone: GL3)	Biolegend	118119; RRID:AB_10896753
PE-labeled TCRγδ (clone: GL3)	Biolegend	118108; RRID:AB_313832
Zombie NIR Viability	Biolegend	77184
Zombie Violet Viability	Biolegend	423114
APC-labeled Ly6G (clone: 1A8)	Biolegend	127614; RRID:AB_2227348
FITC-labeled CD69 (clone: H1.2F3)	Biolegend	104506; RRID:AB_313108
BV650-labeled CD69 (clone: H1.2F3)	Biolegend	104541; RRID:AB_2616934
PE/Cy5-labeled CD62L(clone: MEL-14)	Biolegend	104410; RRID: AB_313097
APC-labeled CCR6 (clone: 29-2L17)	Biolegend	129813; RRID:AB_1877148
BV785-labeled CCR6 (clone: 29-2L17)	Biolegend	129823; RRID:AB_2715923
BV421-labeled CD27 (clone: LG.3A10)	Biolegend	124223; RRID:AB_2565547
APC-labeled IL-17A (clone: TC-11-18H10.1)	Biolegend	506916; RRID:AB_536017
PE-labeled IL-17 (clone: TC-11-18H10.1)	Biolegend	506904; RRID:AB_315463
PE-labeled IFN-γ (clone: XMG1.2)	Invitrogen	12-7311-41; RRID:AB_1907418
FITC-labeled IFN-γ (clone: XMG1.2)	BD Biosciences	554411; RRID:AB_395375
BV711-labeled TCRβ (clone: H57-597)	Biolegend	109243; RRID:AB_2629564
APC/Cy7-labeled CD19 (clone: 6D5)	Biolegend	115529; RRID:AB_830706
APC/Cy7-labeled CD3 (clone: 17A2)	Biolegend	100222; RRID:AB_2057374
ULTRA-LEAF Anti-TCRγδ (clone: UC7-13D5)	Biolegend	107516; RRID:AB_2813964
Bacterial and virus strains		
Streptococcus agalactiae (Group B *Streptococcus*, GBS) COH-1	American Type Culture Collection (ATCC)	COH-1, type III BAA-1176
Escherichia coli BSI-B	Washington University St. Louis, MO	ST131
Chemicals, peptides, and recombinant proteins		
LB broth	Life Technologies	22700041
MacConkey Agar	Fisher Healthcare	OXCM0115B
Tryptic Soy Agar	DIFCO	236950
1X PBS	Life Technologies	121039
RPMI 1640	VWR International LLC	45000-412
Percoll	Sigma-Aldrich	P4937-500
Glutamine	Thermo Fisher Scientific	35050061
Fetal Bovine Serum	Cardinal Healthcare	250517
Penicillin/Streptomycin	Fisher Healthcare	BW09757F
Cell Stimulation Cocktail	Biolegend	423301
Collagenase II	Life Technologies	17101015

(*Continued on next page*)

Continued

REAGENT or RESOURCE	SOURCE	IDENTIFIER
Collagenase IV	Life Technologies	17104019
DNAse I	Sigma-Aldrich	10104159001
Bovine Serum Albumin	Sigma-Aldrich	B4287-5G
Human Serum	Sigma-Aldrich	H4522-100ML
Critical commercial assays		
IL-17 DuoSet ELISA	Fisher Healthcare	DY421-05
IFN-γ ELISAmax	Biolegend	430815
IL-18 DuoSet ELISA	Fisher Healthcare	DY7625-05
Quiagen RNeasy Mini Kit	Quiagen	74106
Deposited data		
Nanostring Analysis	NCBI – Gene Expression Omnibus	GEO: GSE253301
Experimental models: Organisms/strains		
C57BL/6	Jackson Laboratory	Strain #000664
TCRδ-/-	Jackson Laboratory	Strain #002120
Nur77-GFP	Jackson Laboratory	Strain #016617
Software and algorithms		
R (version 4.2.3)	R Core Team (2021). R: A language and environment for statistical computing. R Foundation for Statistical Computing, Vienna, Austria.	https://cran.r-project.org/
ggPlot2	H. Wickham. ggplot2: Elegant Graphics for Data Analysis. Springer-Verlag New York, 2016.	https://ggplot2.tidyverse.org/
ROSALIND	Nanostring Inc.	https://www.rosalind.bio/nanostring
FlowJo (version 10.7.1)	Treestar Inc.	https://www.flowjo.com/
GraphPad PRISM	GraphPad Software Inc.	https://www.graphpad.com/

RESOURCE AVAILABILITY

Lead contact

For further information and access to resources please address the lead contact, Kathryn Knoop (knoop.kathryn@mayo.edu).

Materials availability

Bacterial strains generated in this study are available upon request to Kathryn Knoop (knoop.kathryn@mayo.edu) for *E. coli* BSI-B.

Data and code availability

- NanoString data have been deposited at NCBI Gene Expression Omnibus and are publicly available as of the date of publication. Accession numbers are listed in the key resources table.
- This paper does not report original code.
- Any additional information required to reanalyze the data reported in this paper is available from the lead contact upon request.

EXPERIMENTAL MODEL AND STUDY PARTICIPANT DETAILS

Mice

C57BL/6, TCRδ-/- and Nur77-GFP mice were purchased from The Jackson Laboratory. All animals were bred following the Institutional Animal Care and Use Committee (IACUC) guidelines at Mayo Clinic. Pups were infected on postnatal day 7 (P7) and all sexes were included in the study. Mice were infected intraperitoneally (i.p.) with either a single-organism culture of $2x10^4$ CFU *E. coli* BSI-B (an ST131 sequence type *E. coli*) (Washington University, St. Louis, MO), or $1x10^6$ CFU GBS COH-1 (ATCC) using an insulin syringe (Cardinal Healthcare). Pups were sacrificed 18 hours later. Anti-TCRγδ antibody (UC7-13D5, Biolegend) was given intraperitoneally for *in vivo* blockade of the TCR on γδ T cells (15 μg/g body weight) as described in Figure 1D.

METHOD DETAILS

Preparation of bacteria

Clinical *E. coli* isolates were prepared as described previously,[3] and GBS COH-1 was obtained from ATCC. Single bacterial colonies of GBS and *E. coli* were taken from a streak plate and placed in a 15 mL conical (Fisher Healthcare) containing 5 mL of LB broth (Fisher Healthcare) and placed into a 37°C incubator overnight. The following day, 10 mL of LB broth was measured into a 50 mL conical tube (Fisher Healthcare), and a sterile dropper was used to place 2-3 drops of overnight bacterial stock into fresh LB broth. Bacteria was shaken at 150 rpm at 37°C until an OD of 0.3 was reached. The bacterial culture was spun down at 10200 rpm for 10 minutes (*E. coli*) or 30 minutes (GBS) and the LB supernatant was discarded. The bacterial pellet was resuspended in 10mL of sterile PBS (Life Technologies) and diluted to proper infection dose. To determine *E. coli* and GBS bacterial burden, the liver was harvested and digested in 1mL of sterile PBS (Life Technologies) and 0.5 g of zirconium beads (0.5mm, Fisher Healthcare) in a safe-lock snap cap tube (Fisher Healthcare) and placed into a tissue homogenizer for 5 minutes. The liver homogenate was then serially diluted in sterile PBS (Life Technologies) to achieve a $1:10^5$ dilution (*E. coli*) or $1:10^6$ dilution (GBS). Bacterial homogenate from *E. coli* and GBS-infected pups was plated on either MacConkey agar (Fisher Healthcare) or Tryptic Soy Agar (DIFCO) plates, respectively. CFUs were counted the following day. For heat-killing of bacteria, 1 mL of overnight bacterial stock was placed into an Eppendorf tube (Fisher Healthcare) and placed on a heat block at 55°C for 90 minutes, shaking at 300 rpm.

Enzyme-Linked Immunosorbent Assay (ELISA)

Blood was collected from pups and allowed to clot for 45 minutes at room temperature and spun down at 10,000xg for 2 minutes. The serum was collected and was stored at -20°C until use. ELISAs were performed according to manufacturer's instructions. Serum samples were diluted 1:5 in ELISA diluent buffer (Biolegend). Analysis of serum IL-12 was performed by EVE Technologies (Calgary, AB).

Flow cytometry

Spleens were harvested from mice and were placed in 1 mL of RPMI 1640 (VWR International LLC), and mechanically homogenized using the frosted end of two glass slides (Fisher Healthcare). Spleens were counted using an automated cell counter (Thermo Fisher Scientific). Cells were pelleted and resuspended in 500 μL FACS buffer (PBS containing 5% human serum (Sigma-Aldrich), 0.5% BSA (Sigma-Aldrich), 0.1% sodium azide) and allowed to block for 20 minutes at 4°C. Surface master mix was made in FACS buffer and staining was performed for 30 minutes in the dark at 4°C. Following surface staining, samples were washed twice with FACS buffer and acquired on the CyTek Northern Lights Spectral Flow Cytometer (Cytek Biosciences).

Liver digestion for analysis by flow cytometry

Animals were euthanized and the liver was harvested and placed into 2 mL RPMI containing 1mg/mL of DNAse I (Sigma-Aldrich, INC), Collagenase II (Life Technologies) and Collagenase IV (Life Technologies). The mixture was placed into a gentleMACS C Tube (Miltenyi Biotech) and placed onto an OctoMACS Tissue Dissociator (Miltenyi Biotech) for 30 minutes at 37°C. Samples were then quenched with 8 mL of fresh RPMI (VWR International LLC) and added to a new 15 mL conical tube (Fisher Healthcare). Samples were pelleted at 1500 rpm for 5 minutes before being counted and blocked in 1 mL of FACS buffer. Following blocking, samples were stained for surface markers and acquired on CyTek Northern Lights Spectral Flow Cytometer (CyTek Biosciences).

Intracellular cytokine staining

Cells were placed in 250 μL RPMI supplemented with 10% FBS, 2mM Glutamine (Gibco), 2mM Pyruvate (BioWhittaker), 50 μg/mL Pen/Strep (BioWhittaker), and 0.55 mM 2-ME (Gibco). 1X protein transport inhibitor (Fisher Healthcare) and 1:1000 phorbol 12-myristate 13-acetate (PMA)/Ionomycin (Cell Activation Cocktail, Biolegend) were added, and samples were placed in an incubator at 37°C for four hours. Samples were spun down and resuspended in FACS buffer to block for 15 minutes. Samples were then stained for surface markers for 30 minutes at 4°C before 100 μL of fixative (Life Technologies) was added to each sample for 30 minutes at room temperature. Samples were then washed once with FACS buffer and once with 1X perm buffer (Biolegend) and spun down at 1500 rpm for 5 minutes. Samples were then resuspended in 100 μL 1X perm buffer and intracellular antibodies and were placed at 4°C overnight. The following day, samples were washed twice with FACS buffer and acquired on the CyTek Northern Lights Spectral Flow Cytometer (CyTek Biosciences).

Brain isolation for analysis by flow cytometry

Mice were anesthetized with 10 ug/g of Ketamine/Xylazine mixture and transcardially perfused with 10 mL of cold, sterile PBS (Life Technologies). Brains were digested as previously described.[57] In brief, brains were isolated and placed into a 50 mL conical tube (Fisher Healthcare) containing 5 mL of RPMI (VWR International LLC). The RPMI containing the brains of the mice were then transferred to a 7 mL glass Tenbroeck Dounce homogenizer (Pyrex) and homogenized until the brain was visibly digested (about 10 plunges). The homogenate was then poured through a 70 μm filter into a new 50 mL conical tube, and 10 more mL of RPMI 1640 was added, along with 1 mL of 10X PBS and 9 mL of Percoll (Sigma-Aldrich INC). The 50 mL conical tubes were then placed into a centrifuge and pelleted at 7840xg for 30 minutes at 4°C. Following the spin, the supernatant was fully aspirated off and samples were washed with 50 mL of fresh RPMI 1640 and spun again at 1500 rpm for 10 minutes. Samples were then blocked in FACS buffer for 15 minutes before surface staining was performed at 4°C for 30 minutes.

mRNA isolation from brains

Brains were homogenized in 1 mL of sterile PBS (Life Technologies) using a Tenbroeck Dounce homogenizer (Pyrex). 100 μL of brain homogenate was used for mRNA isolation with the Qiagen RNeasy Mini Kit according to manufacturer's instructions. RNA samples were stored at -80°C until ready for use.

Nanostring

Nanostring nCounter Mouse Immunology Max Kit was used following mRNA isolation from the brain. RNA hybridization was performed according to Nanostring manufacturer's instructions. Samples were incubated for 24 hours at 65°C and then were run on the nCounter Prep Station 5s before being placed on the nCounter Digital Analyzer. Raw and normalized counts were collected from ROSALIND platform. Normalized counts were used for PCA plots, which were plotted using ggplot2 and R version 4.2.3. Log2 fold change and p-values for selected comparisons were calculated by ROSALIND platform. False Discovery Rate was calculated from ROSALIND platform using the Benjamini-Yekutieli calculation for multiple test corrections. Selected comparisons were plotted as volcano plots using ggplot2 and R version 4.2.3. A threshold of > +/-0.6 log2 fold change and p-value of <0.05 was selected for plotting differentially expressed genes.

QUANTIFICATION AND STATISTICAL ANALYSIS

Student's unpaired t-test, One-way ANOVA, and Kaplan-Meier tests were conducted using GraphPad Prism (GraphPad Software, Inc.,). Significance is reported as ns = $p > 0.05$, * = $p \leq 0.05$, ** = $p \leq 0.01$, *** = $p \leq 0.001$, **** = $p \leq 0.0001$.